Available online at www.sciencedirect.com
ScienceDirect
Trans. Nonferrous Met. Soc. China 30(2020) 2650−2657
Transactions of Nonferrous Metals Society of China
www.tnmsc.cn

Microstructure modification and precipitation strengthening for Mg−6Zn−1Mn−4Sn−0.5Ca through extrusion and aging treatment

Xia CHEN[1,2], Ding-fei ZHANG[1,2], Yang ZHAO[1,2], Jing-kai FENG[1,2], Bin JIANG[1,2], Fu-sheng PAN[2,3]

1. College of Materials Science and Engineering, Chongqing University, Chongqing 400045, China;
2. National Engineering Research Center for Magnesium Alloys, Chongqing University, Chongqing 400044, China;
3. Chongqing Academy of Science and Technology, Chongqing 401123, China

Received 8 January 2020; accepted 14 July 2020

Abstract: The microstructure revolution and mechanical properties of as-extruded and peak-aged Mg−6Zn−1Mn−4Sn−0.5Ca (ZMT614−0.5Ca) alloy were studied by OM, SEM, TEM, hardness testing and tensile testing. The results showed that the as-cast ZMT614−0.5Ca alloy mainly consisted of α-Mg, Mg−Zn and CaMgSn phase. The hot extrusion process effectively refined the microstructure and led to a completely dynamic recrystallized microstructure. The average grain size of as-extruded alloy was ~4.85 μm. After solution treatment, remained CaMgSn with high melting point played a significant role in pinning effect and impeding the migration of grain boundary. After aging treatment, peak-aged ZMT614−0.5Ca alloy exhibited a good combination of strength and ductility, with yield strength, ultimate tensile strength and elongation being 338 MPa, 383 MPa and 7.5%, respectively. The yield strength of the alloy increased significantly by around 36% compared with that in as-extruded condition, which should be attributed to the precipitation strengthening of β' phase.

Key words: Mg−6Zn−1Mn−4Sn−0.5Ca; extrusion; aging; microstructure; precipitation strengthening

1 Introduction

Magnesium (Mg) alloys have become an attractive and promising alloys in auto-mobile, aircraft, aerospace, and 3C industries due to their low density (~1/4 of steel and ~3/5 of aluminum), high specific strength, high specific stiffness and good damping ability [1−3]. However, their undesirable strength and ductility, compared with aluminum (Al) alloys and steels, restrict the long-term application prospects of Mg alloys [4,5]. It is well known that alloying is an effective method to enhance mechanical properties by changing the grain size, precipitates and texture of magnesium alloys. And developing high strength and rare earth-free magnesium (Mg) alloys is a long-term goal in the field of light alloys, so many non-rare earth elements have been added into Mg to strengthen Mg alloys including Zn, Al, Sn and Ca, etc [6−8].

Mg−Zn alloys containing 4−9wt.%Zn have an excellent age-hardening ability due to the precipitation of transition phases [9−11]. Semi-metal Sn is regarded as an alloying element to effectively modify the microstructure of Mg−Zn alloys. Formation of the high melting point intermetallic compound of Mg_2Sn can improve the mechanical properties of Mg alloys at elevated temperatures [12−16]. Sn addition to Mg−Zn alloy can not only refine the β precipitates during aging, but also promote the formation of dense and fine Mg_2Sn precipitates [16]. In our previous study, the

Foundation item: Project (2016YFB0301101) supported by the National Key Research and Development Program of China; Projects (51571040, U1764253, 51531002) supported by the National Natural Science Foundation of China
Corresponding author: Ding-fei ZHANG; Tel: +86-23-65112491; E-mail: zhangdingfei@cqu.edu.cn
DOI: 10.1016/S1003-6326(20)65409-7

effects of Sn on Mg−6Zn−1Mn (ZM61) alloy have been studied and Mg−6Zn−1Mn−4Sn (ZMT614) alloy was found to own the best mechanical properties in Mg−6Zn−1Mn−*x*Sn (*x*=1, 2, 4, 6, 8, 10) [17]. In addition, Ca element, with a high growth restriction factor (GRF), is regarded as a very attractive and cheap element to refine grain size [18]. Mg−Zn−Ca series alloys have been widely researched and found that Ca addition to Mg alloy can effectively weaken the basal texture and refine the microstructure [19,20]. CHANG et al [21] also found that Ca refines the micro-sized and nano-sized Mg_2Sn when added into Mg−5Sn−3Zn alloy. ZHANG et al [22] also found that Mg−6Sn alloy was refined with the addition of Zn and Ca elements. PAN et al [23] developed TX22 which was low-alloyed and rare earth-free magnesium alloys with ultra-high strength. The Ca addition promoted accumulation of the pyramidal dislocations, and the soluted Ca segregation and nano-precipitates can block the motion of LAGBs. The effects of Zn to Sn mass ratio [24,25] and minor Ca addition [26] on the microstructure and mechanical properties of Mg−Zn−Sn−Al-based alloys have also been studied. Minor Ca addition can effectively refine both grains and grain-boundary compounds, and addition of Ca improved the strength of the Mg−Zn−Sn−Al alloy, but decreased the ductility. Therefore, Sn and Ca are potential elements for Mg−Zn alloys. However, no detailed research has been conducted on the microstructures and mechanical properties of ZMT614−Ca. Therefore, we developed a new high strength Mg−6Zn−1Mn−4Sn−0.5Ca alloy.

The aim of this work is to investigate the microstructure and properties of as-extruded and heat-treated Mg−6Zn−1Mn−4Sn−0.5Ca alloy using optical microscopy (OM), X-ray diffractometer (XRD), scanning electron microscopy (SEM), transmission electron microscopy (TEM), hardness tests and uniaxial tensile tests.

2 Experimental

The alloy with actual chemical compositions of Mg−5.89Zn−0.77Mn−3.85Sn−0.48Ca was prepared with commercially pure Mg (>99.9 wt.%), Zn (>99.95 wt.%), Sn (>99.9 wt.%), Mg−2.7Mn (2.7 wt.%) and Mg−30Ca (30.0 wt.%) master alloy. All the raw materials were melted at about 730 °C in a ZG−0.01 vacuum induction melting furnace in an Ar gas atmosphere. The actual chemical compositions of alloy were tested by XRF−800 CCDE X-ray fluorescence spectrometer. The original billet was a cylinder with a diameter of 90 mm. The cast ingots were then homogenized at 330 °C for 14 h and 420 °C for 2 h. Before the ingots were extruded, both the ingots and extrusion die were heated to 350 °C for 60 min. The ingots were extruded at 350 °C with an extrusion ratio of 25:1 and a ram speed of 12 mm/s. Then the extruded bars were solution-treated at 420 °C for 2 h in air atmosphere followed by water quenching (T4). After solution treatment, the following artificial aging treatments (T6) were performed. The aging treatment was carried out at 180 °C from 0 to 100 h. Hardness measurements were performed by a micro-Vickers apparatus under a load of 50 g.

The average size of grains was calculated by the software of Image-Pro using an average linear intercept method. Optical microscopy (OM) and scanning electron microscopy (SEM) observations were carried out on an OLYMPUS LEXT OLS4000 optical microscope and a JEOL JSM−7800F scanning electron microscope equipped with an energy dispersive X-ray spectrometer (EDS), respectively. Electron backscattered diffraction (EBSD) analysis was conducted to analyze the microstructure and micro-textures of the as-extruded alloy. Transmission electron microscopy (TEM) observations were performed on an FEI Tecnai G2 F20. Phase analysis was determined by a Rigaku D/max2500PC X-ray diffractometer (XRD) using a Cu K_α radiation with a scanning angle from 10° to 90° and a scanning rate of 4 (°)/min. For OM and SEM observations, the specimens were prepared by grinding with 400−1200 grit SiC papers, then etched with a mixture of 1 g picric acid, 1 mL acetic and 8 mL ethanol. For EBSD observation, the specimens were ground followed by electrolytic polishing. Tensile tests were carried out at room temperature using a SANS CMT−5105 electronic universal testing machine at a strain rate of $\sim 1\times10^{-3}$ s^{-1} with a gauge length of 35 mm and a cross-sectional diameter of 5 mm. Three samples at least were tested for each condition.

3 Results and discussion

3.1 Microstructure of tested alloy

Figure 1 shows the XRD pattern and analysis results of the as-cast alloy. The main phase for ZMT614−0.5Ca alloy consists of α-Mg, MgZn, and CaMgSn. No Mg_2Ca is found, which depends on the mass ratio of Sn to Ca in the alloy, with a critical transition value in the range of 3:1−3.5:1 [25]. In this study, the mass ratio of Sn to Ca for ZMT614−0.5Ca alloy is about 8/1 which is much higher than the critical value. In addition, the electronegative values of Mg, Zn, Sn and Ca are 1.31, 1.96, 1.65, and 1.00, respectively. The electronegativity difference between Ca and Sn is the highest among all the elements, implying that Ca and Sn are more likely to form CaMgSn ternary phase. So, Ca element is consumed firstly by Sn element.

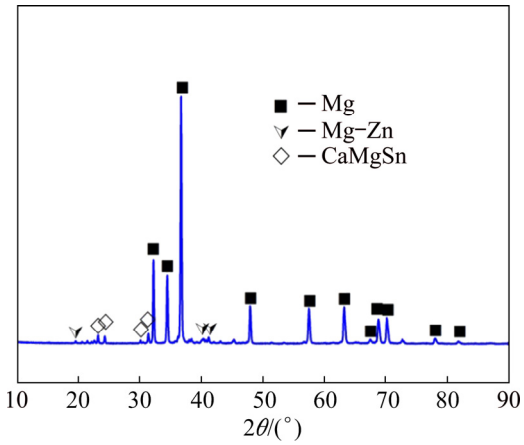

Fig. 1 XRD pattern of as-cast alloy

SEM images of the as-cast alloy are shown in Fig. 2. The white eutectic phase is MgZn according to the EDS results in Table 1. Point *A* is enriched with Ca, Sn and Mg elements, so this needle-like phase could be related to CaMgSn, which can also be supported by the XRD results.

Optical image of as-homogenized ZMT614−0.5Ca alloys is presented in Fig. 3. Some eutectic compounds can be dissolved by homogenization, which improves the uniformity of the microstructure and the formability of the alloy. A large proportion of Mg−Zn eutectic compound dissolves during homogenization, resulting in the gray transition area which is mainly composed of a large number of particle phases. This is because

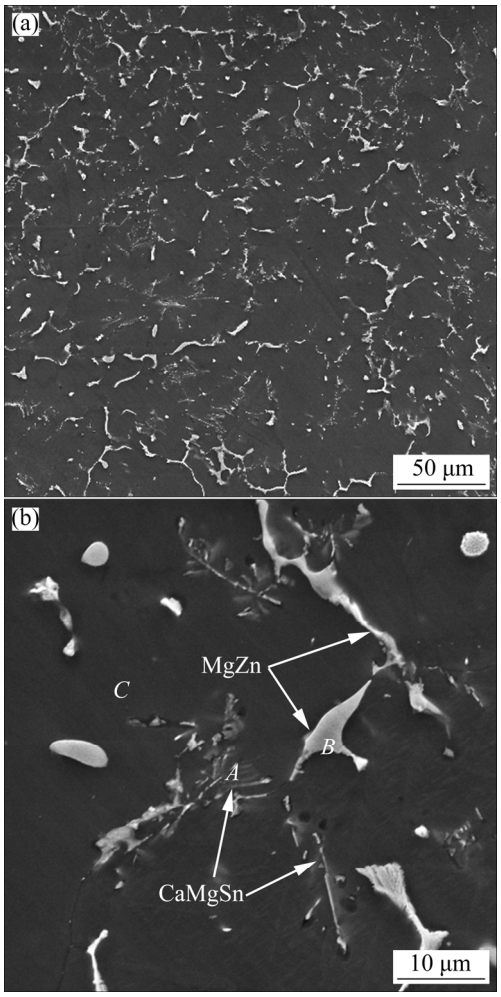

Fig. 2 SEM images of as-cast alloy

Table 1 EDS results of as-cast alloy in Fig. 2(b) (at.%)

Point	Mg	Zn	Ca	Sn	Mn
A	72.70	19.18	4.88	3.27	
B	68.80	31.05	0.16	−	
C	77.78	20.02	0.04	−	2.17

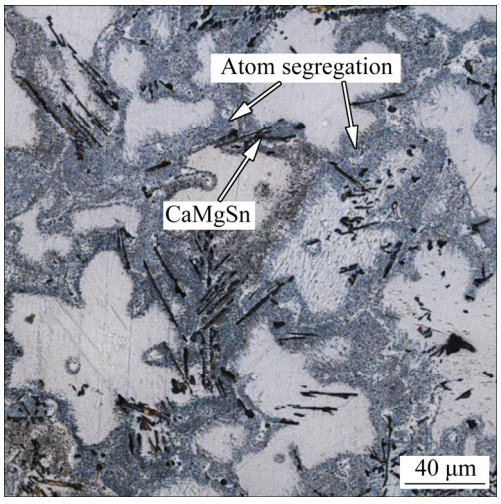

Fig. 3 Optical image of homogenized alloy

Mg−Zn eutectic phases diffuse to poor Zn dendrite areas, resulting in the zinc-rich area near grain boundaries. Almost all of CaMgSn still remains as needle-shape and no dissolution occurs. As is reported, CaMgSn is a thermal stable phase with a high melting point (over 1000 °C) [27,28].

Figure 4 shows the OM, SEM and TEM images of extruded ZMT614−0.5Ca alloys. Undissolved phases are fractured into particles with several micrometers along the extrusion direction (ED) during hot extrusion. Completly dynamic recrystallized (DRXed) microstructure forms in as-extruded alloy due to plenty of micron-sized second phases working as nucleation sites, which promote the dynamic recrystallization. The average grain size of recrystallized grains for extruded alloy is about 4.85 μm. Needle-like CaMgSn turns into short rods as shown in Fig. 4(b). Fine spherical precipitates (Fig. 4(c)) observed in TEM image indicate that dynamic precipitation occurs, which is induced by supersaturated solution atoms in the matrix.

Figure 5(a) shows the inverse pole figure. Most grains are shown as red color, indicating that these grains are oriented with normal direction of (0001) basal plane perpendicular to the extrusion direction (ED). The (0001) and $(10\bar{1}0)$ pole figures measured by EBSD for the extruded alloy are shown in Fig. 5(b). The texture of the alloy is a typical extruded basal texture and the intensity of maximum texture intensity is 7.16. Figure 5(c) shows the (0001) Schmid factor distribution of extruded ZMT614−0.5Ca alloys. When the applied load reaches the critical resolved shear stress (CRSS) of basal slip of Mg alloy, the slip systems on basal plane are activated. And the CRSS of basal

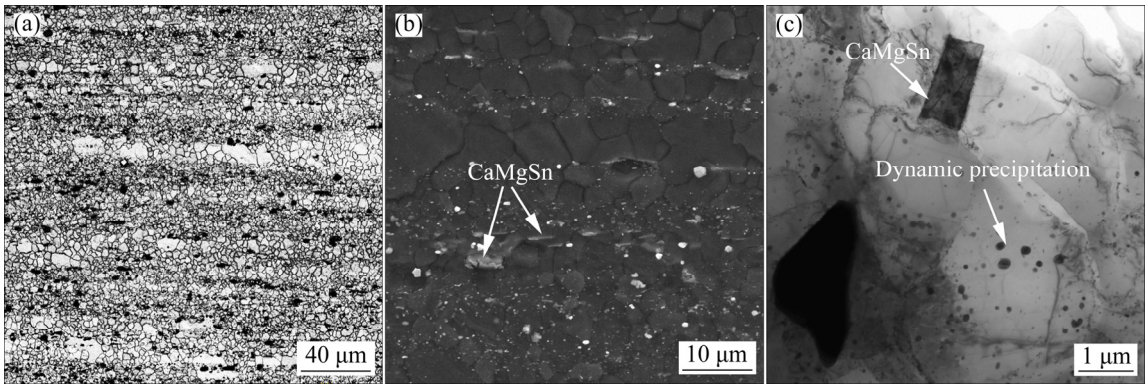

Fig. 4 OM (a), SEM (b) and TEM (c) images of as-extruded alloy

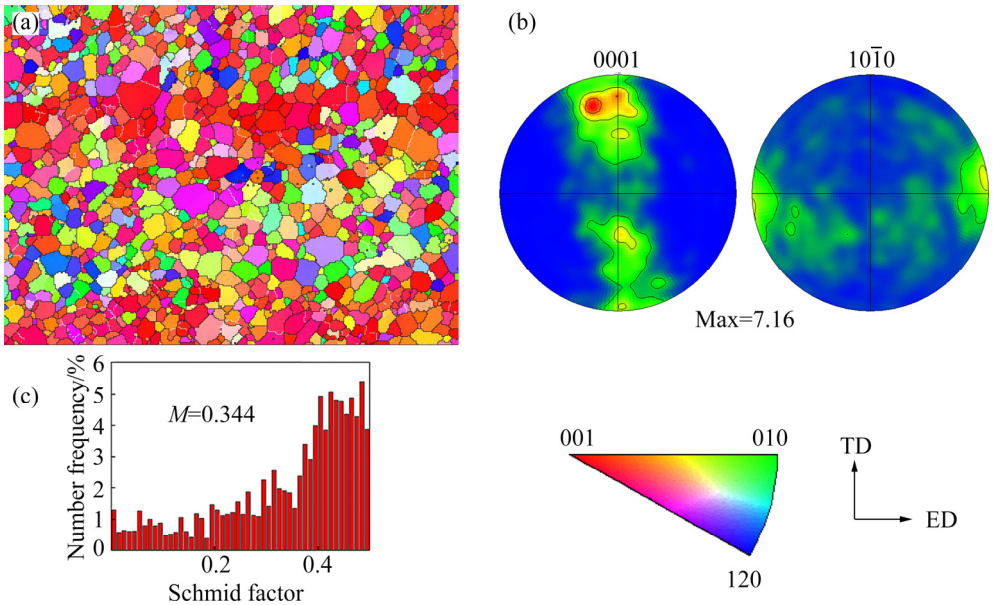

Fig. 5 Inverse pole figure (a), (0001) and $(10\bar{1}0)$ pole figures (b) and Schmid factor distribution measured by EBSD (c) for as-extruded alloy

slip depends on the orientation factor or Schmid factor whose value is between 0 and 0.5. If the value is close to 0, the slip systems are difficult to be activated. If the value is close to 0.5, the slip systems are easy to be activated [19,29]. In this study, the Schmid factor of (0001) plane is about 0.344. This implies that orientation of most grains is conducive to (0001) basal slip, which contributes to the deformation.

To dissolve most second phase into the matrix at high temperatures, and to form the supersaturated solid solution at room temperature, solution treatment is carried out [30]. The microstructure of the solution-treated alloy is shown in Fig. 6, and the average grain size increases to 21.6 μm during solution treatment. CaMgSn still remains and these residual phases play a significant role in pinning effect and impeding the migration of grain boundary with the heat-treatment.

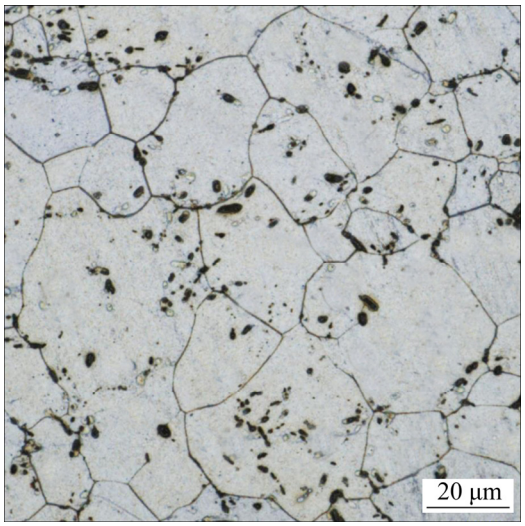

Fig. 6 OM image of solution-treated alloy

The bright field TEM images of the peak-aged alloy are presented in Fig. 7. Plenty of rod precipitates parallel to $[0001]_{Mg}$ direction and plate precipitates perpendicular to $[0001]_{Mg}$ are found. Based on the previous studies [31−33] and selected area electron diffraction (SAED) pattern in Fig. 7(b), we can conclude that the two precipitates are rod-like β' and disc-like β'', and β' is still the primary precipitates during aging in this alloy. The precipitation in aging treatment is obviously different from dynamic precipitation in extrusion process. Aging precipitation phases are fine and precipitated on the certain direction of habit plane.

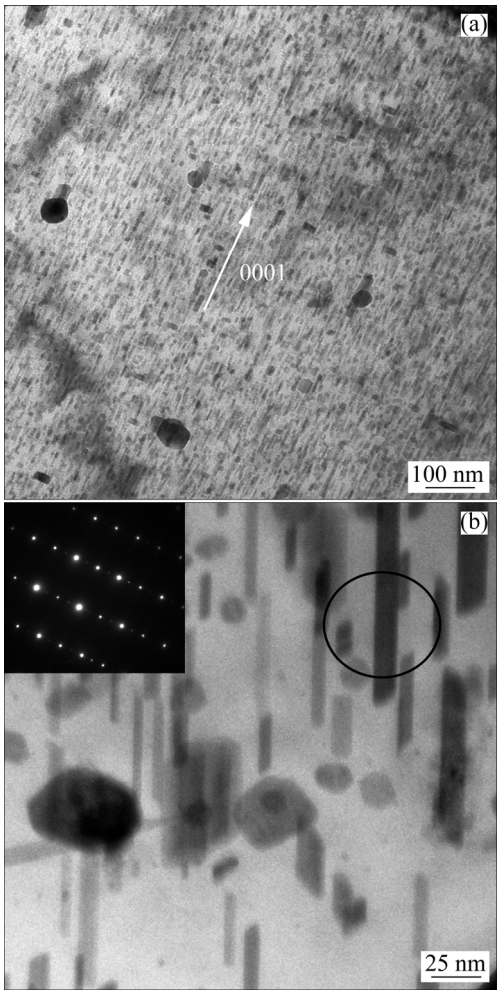

Fig. 7 Bright field TEM images of peak-aged alloy taken from $[11\bar{2}0]_{Mg}$

3.2 Mechanical properties of tested alloy

Figure 8 shows the age-hardening curve of the aged alloy at 180 °C. The hardness of as-extruded alloy is HV 74.8. After solution treatment, the hardness of the alloy decreases to HV 66. As the aging time increases, the hardness increases rapidly to the peak value with HV 94 after ~6 h. Then the hardness decreases slowly. The reason for the increase in hardness is the precipitated phases during the aging process.

Figure 9(a) shows the stress−strain curves of extruded and peak-aged ZMT614−0.5Ca alloy. Figure 9(b) summarizes the tensile properties of alloy in two states. For the as-extruded alloys, the yield strength (YS), ultimate tensile strength (UTS), and the elongation-to-failure (EL) of the alloy are 249, 338 MPa and 13.6%, respectively. The balanced mechanical properties have a close relation with the complete DRXed microstructure,

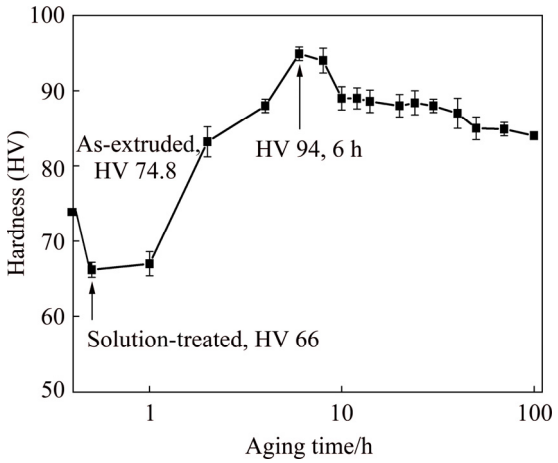

Fig. 8 Age-hardening curve of ZMT614−0.5Ca alloy treated at 180 °C

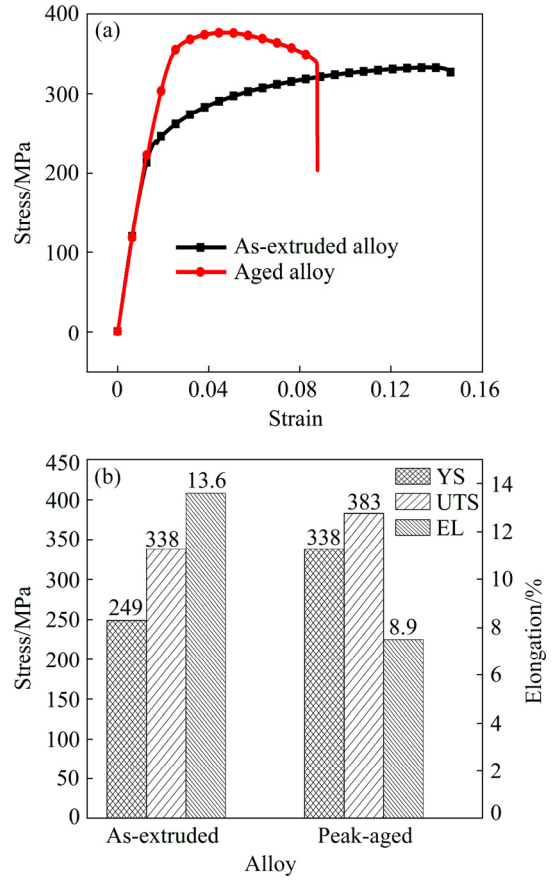

Fig. 9 Tensile properties of as-extruded and peak-aged alloys

dislocations and dynamic precipitation during deformation.

The strength of the alloy rises sharply after the aging treatment, and the yield strength increases to 338 MPa and the ultimate strength increases to 383 MPa at a small penalty in elongation with 7.5%. Generally, the enhancement of yield strength of magnesium alloy can be attributed to the grain refinement, precipitation strengthening and solid-solution strengthening [33,34]. While the grains become coarser which would weaken the YS and UTS according to the Hall−Petch relationship [35]. Besides, the solute element reduced during heat treatment. Therefore, the significant improvement of YS of the aged alloy should be attributed to the precipitation strengthening, and the favorable factor outweighs the two negative factors.

As we all know, basal slip system is the easiest slip system for Mg alloys. Rod β' precipitates perpendicular to the basal plane are very helpful to block the dislocation movement on the base plane. According to the Orowan equations, NIE [35] has built a model for contribution to precipitation strengthening of the (0001) Mg rods as follows:

$$\sigma_{\mathrm{ppt}}=\frac{Gb}{2\pi(1-\nu)^{1/2}\left(\dfrac{0.953}{f_{\mathrm{v}}^{1/2}}-1\right)d_{\mathrm{t}}}\ln\frac{d_{\mathrm{t}}}{b}$$

where G is the shear modulus of the Mg matrix, b is the magnitude of the burgers vector, ν is Poisson ratio, f_{v} is the triangular prismatic volume fraction of the precipitates and d_{t} is the mean diameter of the precipitates. It should be noted that σ_{ppt} is dependent on f_{v}. As shown in Fig. 7, the volume of β' in ZMT614−0.5Ca alloy substantially rises in the peak aged condition, which results in the increase of f_{v}. Therefore, the YS is improved significantly for ZMT614−0.5Ca alloy.

The sharp decrease of elongation after aging treatment should be attributed to the following reasons. The first one is the coarsening of grains. It is widely accepted that grain refinement is good for the elongation of alloy because the plastic deformation of fine grains under external load can be coordinated in many grains, then the plastic deformation is more uniform, thus the stress concentration is smaller. While the increase of grain size after solution and aging treatment for ZMT614−0.5Ca alloy weakens the capacity of strain accommodation between grains. Secondly, consumption of solute element and formation of precipitates are also responsible for the decrease of elongation. The aging treatment leads to the depletion of solute element and deactivates solution softening of the prismatic slip, which plays a role in accommodating local deformation incompatibility [36]. Besides, the decrease of solute element is deemed to improve the stacking fault

energy [37], which restricts the dislocation dissociation and promotes cross-slip, thus weakening the dislocation-storage capabilities and lower hardening rate, so a lower homogeneous elongation is obtained.

4 Conclusions

(1) The cast Mg−6Zn−1Mn−4Sn−0.5Ca alloy mainly consisted of α-Mg, Mg−Zn and CaMgSn phase. The grains were refined during hot extrusion and a completely dynamic recrystallized microstructure formed. The average grain size of extruded alloy was ~4.85 μm.

(2) During aging treatment, the hardness increased rapidly to the peak value after ~6 h. β' was still the primary precipitates during aging.

(3) After aging treatment, peak-aged Mg−6Zn−1Mn−4Sn−0.5Ca alloy exhibited a good combination of strength and ductility, with yield strength, ultimate tensile strength and elongation being 338 MPa, 383 MPa and 7.5%, respectively. The yield strength of the alloy increased significantly by around 36% compared with that in as-extruded condition, which should be attributed to the precipitation strengthening.

References

[1] ZHAO Hong-liang, HUA Yun-xiao, DONG Xiang-lei, XING Hui, LU Yan-li. Influence of trace Ca addition on texture and stretch formability of AM50 magnesium alloy sheet [J]. Transactions of Nonferrous Metals Society of China, 2020, 30(3): 647−656.

[2] YOU Si-hang, HUANG Yuan-ding, KAINER K U, HORT N. Recent research and developments on wrought magnesium alloys [J]. Journal of Magnesium and Alloys, 2017, 5(3): 239−253.

[3] HUANG Lun, HUANG Guang-sheng, DENG Qian-yuan, TANG Ai-tao, JIANG Bin, PAN Fu-sheng. Effects of trace Ce and Ca on microstructure evolution and formability of AZ31 alloys [J]. The Chinese Journal of Nonferrous Metals, 2019, 29(3): 429−438. (in Chinese)

[4] PAN Hu-cheng, REN Yu-ping, FU He, ZHAO Hong, WANG Li-qing, MENG Xiang-ying, QIN Gao-wu. Recent developments in rare-earth free wrought magnesium alloys having high strength: A review [J]. Journal of Alloys and Compounds, 2016, 663: 321−331.

[5] DAMAVANDI E, NOUROUZI S, RABIEE S M, JAMAATI R. Effect of ECAP on microstructure and tensile properties of A390 aluminum alloy [J]. Transactions of Nonferrous Metals Society of China, 2019, 29(5): 931−940.

[6] WEI Jie, WANG Qu-dong, ZHANG Li, YIN Dong-di. Microstructure refinement of Mg−Al−RE alloy by Gd addition [J]. Materials Letters, 2019, 246: 125−128.

[7] BAE S W, KIM S H, LEE J U, JO W K, HONG W H, KIM W, PARK S H. Improvement of mechanical properties and reduction of yield asymmetry of extruded Mg−Al−Zn alloy through Sn addition [J]. Journal of Alloys and Compounds, 2018, 766: 748−758.

[8] WANG Feng, DONG Hai-kuo, SUN Shi-jie, WANG Zhi, MAO Ping-li, LIU Zheng. Microstructure, tensile properties, and corrosion behavior of die-cast Mg−7Al−1Ca−*x*Sn alloys [J]. Journal of Materials Engineering and Performance, 2018, 27(2): 612−623.

[9] WEI L Y, DUNLOP G L, WESTENGEN H. Precipitation Hardening of Mg−Zn and Mg−Zn−RE alloys [J]. Metallurgical and Materials Transactions A, 1995, 26(7): 1705−1716.

[10] WU Hai-rong, DU Wen-bo, LI Shu-bo, LIU Ke, WANG Zhao-hui. Microstructure and mechanical properties of AZ31 magnesium alloy reinforced by *I*-phase [J]. Rare Metals, 2019, 38(8): 733−738.

[11] JANG H S, LEE B J. Effects of Zn on <*c*+*a*> slip and grain boundary segregation of Mg alloys [J]. Scripta Materialia, 2019, 160: 39−43.

[12] SHI Zhang-zhi, ZHANG Min, HUANG Xue-fei, LIU Xue-feng, ZHANG Wen-zheng. Research progress in age-hardenable Mg−Sn based alloys [J]. Acta Metallurgica Sinica, 2019, 55: 1231−1242. (in Chinese)

[13] SASAKI T T, OH-ISHI K, OHKUBO T, HONO K. Effect of double aging and microalloying on the age hardening behavior of a Mg−Sn−Zn alloy [J]. Materials Science and Engineering A, 2011, 530: 1−8.

[14] WEI Shang-hai, ZHU Tian-ping, HODGSON M, GAO Wei. Effects of Sn addition on the microstructure and mechanical properties of as-cast, rolled and annealed Mg−4Zn alloys [J]. Materials Science and Engineering A, 2013, 585: 139−148.

[15] ZOU Jian-kun, CHEN Ji-hua, YAN Hong-ge, XIA Wei-jun, SU Bin, LEI Yi, WU Qin. Effects of Sn addition on dynamic recrystallization of Mg−5Zn−1Mn alloy during high strain rate deformation [J]. Materials Science and Engineering A, 2018, 735: 49−60.

[16] WEI Shang-hai, ZHU Tian-ping, HOU Hai-bo, KIM J H, KOBAYASHI E, SATO T, HODGSON M, GAO Wei. Effects of Pb/Sn additions on the age-hardening behaviour of Mg−4Zn alloys [J]. Materials Science and Engineering A, 2014, 597: 52−61.

[17] QI Fu-gang, ZHANG Ding-fei, ZHANG Xiao-hua, XU Xing-xing. Effect of Sn addition on the microstructure and mechanical properties of Mg−6Zn−1Mn (wt.%) alloy [J]. Journal of Alloys and Compounds, 2014, 585: 656−666.

[18] ALI Y, QIU Dong, JIANG Bin, PAN Fu-sheng, ZHANG Ming-xing. Current research progress in grain refinement of cast magnesium alloys: A review article [J]. Journal of Alloys and Compounds,2015, 619: 639−651.

[19] TU Teng, CHEN Xian-hua, CHEN Jiao, ZHAO Chao-yue, PAN Fu-sheng. A high-ductility Mg−Zn−Ca magnesium alloy [J]. Acta Metallurgica Sinica (English Letter), 2019, 32(1): 23−30.

[20] DU Y Z, QIAO X G, ZHENG M Y, WANG D B, WU K, GOLOVIN I S. Effect of microalloying with Ca on the microstructure and mechanical properties of Mg−6 mass% Zn alloys [J]. Materials & Design, 2016, 98: 285−293.

[21] CHANG L L, TANG H, GUO J. Strengthening effect of nano and micro-sized precipitates in the hot-extruded Mg−5Sn−3Zn alloys with Ca addition [J]. Journal of Alloys and Compounds, 2017, 703: 552−559.
[22] ZHANG Yang, CHEN Xiao-yang, LU Yan-lin, LI Xiao-ping. Microstructure and mechanical properties of as-extruded Mg−Sn−Zn−Ca alloy with different extrusion ratios [J]. Transactions of Nonferrous Metals Society of China, 2018, 28(11): 219−2198.
[23] PAN Hu-cheng, QIN Gao-wu, HUANG Yun-miao, REN Yu-ping, SHA Xue-chao, HAN Xiao-dong, LIU Zhi-quan, LI Cai-fu, WU Xiao-lei, CHEN Hou-wen, HE Cong, CHAI Lin-jiang, WANG Yun-zhi, NIE Jian-feng. Development of low-alloyed and rare-earth-free magnesium alloys having ultra-high strength [J]. Acta Materialia, 2018, 149: 350−363.
[24] KOZLOV A, OHNO M, ARROVAVE R, LIU Z K, SCHMID-FETZER R. Thermodynamics and solidification microstructures of Mg−Sn−Ca alloys, Part 1: Experimental investigation and thermodynamic modeling of the ternary Mg−Sn−Ca system [J]. Intermetallics, 2008, 16(2): 299−315.
[25] KOZLOV A, OHNO M, LEIL TA, HORT N, KAINER K U, SCHMID-FETZER R. Phase equilibria, thermodynamics and solidification microstructures of Mg−Sn−Ca alloys, Part 2: Prediction of phase formation in Mg-rich Mg−Sn−Ca cast alloys [J]. Intermetallics, 2008, 16(2): 316−321.
[26] HE Xi, CHEN Ji-hua, YAN Hong-ge, SU Bin, ZHANG Guang-hao, MIAO Chong-ming. Effects of minor Ca addition on microstructure and mechanical properties of the Mg−4.5Zn−4.5Sn−2Al-based alloy system [J]. Journal of Alloys and Compounds, 2013, 548: 52−59.
[27] LU Xing, ZHAO Guo-qun, ZHOU Ji-xue, ZHANG Chun-sheng, SUN Lu. Effect of extrusion speeds on the microstructure, texture and mechanical properties of high-speed extrudable Mg−Zn−Sn−Mn−Ca alloy [J]. Vacuum, 2018, 157: 180−191.
[28] WAHID Shah-abdul, LIM Hyun-kyn, JUNG Young-gil, YANG Won-seok, HA Seong-ho, YOON Young-ok, KIM Shae-k. Effect of CaMgSn ternary phase on the aging response of Mg−Sn−Zn−Ca alloys [J]. Journal of Korea Foundry Society, 2018, 38: 75−81.
[29] BHATTACHARJEE T, MENDIS C L, OH-ISHI K, OHKUBO T, HONO K. The effect of Ag and Ca additions on the age hardening response of Mg−Zn alloys [J]. Materials Science and Engineering A, 2013, 575: 231−240.
[30] CHEN Jun-xiu, GAO Ming, TAN Li-li, YANG Ke. Microstructure, mechanical and biodegradable properties of a Mg−2Zn−1Gd−0.5Zr alloy with different solution treatments [J]. Rare Metals, 2019, 38(6): 532−542.
[31] NIE J F, MUDDLE B C. Characterisation of strengthening precipitate phases in a Mg−Y−Nd alloy [J]. Acta Materialia, 2000, 48(8): 1691−1703.
[32] SINGH A, TSAI A P. Structural characteristics of precipitates in Mg−Zn-based alloys [J]. Scripta Materialia, 2007, 57(10): 941−944.
[33] HU Guang-shan, ZHANG Ding-fei, TANG Tian, SHEN Xia, JIANG Lu-yao, XU Jun-yao, PAN Fu-sheng. Effects of Nd addition on microstructure and mechanical properties of Mg−6Zn−1Mn−4Sn alloy [J]. Materials Science and Engineering A, 2015, 634: 5−13.
[34] YANG M B, CHENG L, PAN F S. Effects of calcium addition on as-cast microstructure and mechanical properties of Mg−5Zn−5Sn alloy [J]. Transactions of Nonferrous Metals Society of China, 2010, 20(5): 769−775.
[35] NIE Jian-feng. Precipitation and hardening in magnesium alloys [J]. Metallurgical and Materials Transactions A, 2012, 43: 3891−3939.
[36] ZHANG Jing, DOU Yu-chen, LIU Guo-bao, GUO Zheng-xiao. First-principles study of stacking fault energies in Mg-based binary alloys [J]. Computational Materials Science, 2013, 79: 564−569.
[37] WANG Cong, LUO Tian-jiao, LIU Yun-teng, LIN To, YANG Yuan-sheng. Microstructure and mechanical properties of Mg−5Zn−3.5Sn−1Mn−0.5Ca−0.5Cu alloy [J]. Materials Characterization, 2019, 147: 406−413.

Mg−6Zn−1Mn−4Sn−0.5Ca 合金在挤压和时效过程中的组织演变和析出强化

陈 霞[1,2]，张丁非[1,2]，赵 阳[1,2]，冯靖凯[1,2]，蒋 斌[1,2]，潘复生[2,3]

1. 重庆大学 材料科学与工程学院，重庆 400045；
2. 重庆大学 国家镁合金材料工程技术研究中心，重庆 400044；3. 重庆市科学技术研究院，重庆 401123

摘 要：采用光学显微镜、扫描电子显微镜、透射电镜、硬度试验和拉伸试验对 Mg−6Zn−1Mn−4Sn−0.5Ca (ZMT614−0.5Ca)合金在挤压态和时效态的组织变化及力学性能进行研究。结果表明：铸态 ZMT614−0.5Ca 合金主要包含 α-Mg、Mg−Zn 和 CaMgSn 相。热挤压过程有效地细化晶粒且形成完全动态再结晶组织。挤压态合金的平均晶粒尺寸约为 4.85 μm。固溶处理后，高熔点 CaMgSn 仍然存在，起着重要的钉扎作用和阻碍晶界移动。时效处理后，合金 ZMT614−0.5Ca 具有良好的综合力学性能，屈服强度、抗拉强度和伸长率分别为 338 MPa、383 MPa 和 7.5%。和挤压态相比，合金屈服强度提升约 36%，其主要原因是时效过程 β 相的析出强化。

关键词：Mg−6Zn−1Mn−4Sn−0.5Ca；挤压；时效；显微组织；析出强化

(Edited by Xiang-qun LI)